A Circularly Symmetric Antenna Design With High Polarization Purity and Low Spillover

C. M. Holler, A. C. Taylor, M. E. Jones, O. G. King, S. J. C. Muchovej, M. A. Stevenson, R. J. Wylde, C. J. Copley, R. J. Davis, T. J. Pearson and A. C. S. Readhead

arXiv:1111.2702v3 [astro-ph.IM] 28 Aug 2012

***Abstract*—We describe the development of two circularly symmetric antennas with high polarization purity and low spillover. Both were designed to be used in an all-sky polarization and intensity survey at 5 GHz (the C-Band All-Sky Survey, C-BASS). The survey requirements call for very low cross-polar signal levels and far-out sidelobes. Two different existing antennas, with 6.1-m and 7.6-m diameter primaries, were adapted by replacing the feed and secondary optics, resulting in identical beam performances of 0.73° FWHM, cross-polarization better than -50 dB, and far-out sidelobes below -70 dB. The polarization purity was realized by using a symmetric low-loss dielectric foam support structure for the secondary mirror, avoiding the need for secondary support struts. Ground spill-over was largely reduced by using absorbing baffles around the primary and secondary mirrors, and by the use of a low-sidelobe profiled corrugated feedhorn. The 6.1-m antenna and receiver have been completed and tested. Results show that the co-polar beam matches the design simulations very closely in the main beam and down to levels of -80 dB in the backlobes. With the absorbing baffles in place the far-out ($> 100°$) sidelobe response is reduced below -90 dB. Cross-polar response could only be measured down to a noise floor of -20 dB but is also consistent with the design simulations. Temperature loading and groundspill due to the secondary support were measured at less than 1 K.**

***Index Terms*—Reflector antennas, Antenna measurements, Antenna radiation patterns, Radio Astronomy.**

I. Introduction

Manuscript received November 10, 2011; revised March 21, 2012

This work was supported by NSF grants AST-0607857 and AST-1010024, and by the University of Oxford Department of Physics. A. C. Taylor acknowledges support from a Royal Society Dorothy Hodgkin Fellowship.

C. M. Holler was with the Subdepartment of Astrophysics, Department of Physics, Oxford University, Denys Wilkinson Building, Oxford OX1 3RH, UK and is now with University of Applied Sciences Esslingen, Kanalstrasse 33, 73728 Esslingen am Neckar, Germany (phone: +49-7161-6791269 fax: +49-7161-6792177 e-mail: christian.holler@hs-esslingen.de).

M. E. Jones and A. C. Taylor are with the Subdepartment of Astrophysics, Department of Physics, Oxford University, Denys Wilkinson Building, Oxford OX1 3RH, UK (e-mail: mike@astro.ox.ac.uk and act@astro.ox.ac.uk).

O. G. King, T. J. Pearson, A. C. S. Readhead and M. A. Stevenson are with the Department of Astronomy, California Institute of Technology, Pasadena, 91125, USA (e-mail: ogk@astro.caltech.edu, tjp@astro.caltech.edu, acr@astro.caltech.edu and mas@astro.caltech.edu).

S. J. C. Muchovej is with the Owens Valley Radio Astronomy Observatory, California Institute of Technology, Pasadena, 91125, USA (e-mail: sjcm@astro.caltech.edu).

R. J. Wylde is with the School of Physics and Astronomy, University of St Andrews, Fife, UK and Thomas Keating Ltd, Billingshurst, West Sussex, RH14 9SH, UK (e-mail: r.wylde@terahertz.co.uk).

C. J. Copley was with the Department of Physics and Electronics, Rhodes University, Artillery Road, Grahamstown, South Africa and is now with the Subdepartment of Astrophysics, Department of Physics, Oxford University, Denys Wilkinson Building, Oxford OX1 3RH, UK (e-mail: Charles.Copley@astro.ox.ac.uk).

R. J. Davis is with the Jodrell Bank Centre for Astrophysics, University of Manchester, Manchester, M13 9PL, UK (e-mail: rjd@jb.man.ac.uk).

TOTAL-POWER radio-astronomical imaging, in which an image is formed by scanning a single antenna beam over the sky, presents some of the most stringent possible requirements on antenna design. Accurate measurements require extreme stability of the receiver system as well as minimization of scan-synchronous pickup via sidelobes and cross-polarization response. Such effects are difficult or impossible to remove in post-processing, and drive the need to limit the intrinsic sidelobe response and cross-polarization of the antenna used for total-power imaging. Interferometers are less sensitive to these effects and are typically used for high-resolution radio imaging, but they are insensitive to scales larger than the antenna beam. Large-scale (and in particular, all-sky) images are only attainable by scanning single-dish telescopes. In this paper, we describe the development of two antennas for a sensitive, all-sky imaging experiment, which are designed to have very low levels of sidelobes and cross-polarization.

The C-Band All-Sky Survey (C-BASS) [1], is a project to image the whole sky at 5 GHz in both intensity and polarization, in order to meet a variety of scientific goals in the study of the cosmic microwave background (CMB) radiation and emission processes in the Galaxy. C-BASS will be the first survey of diffuse Galactic emission at a frequency low enough to be dominated by synchrotron radiation but high enough to be largely uncorrupted by Faraday rotation effects. The maps produced by the survey will enable accurate subtraction of foreground contaminating signals from higher-frequency CMB polarization sky surveys, including the *WMAP* [2] and *Planck* [3] satellites, and will also be a major resource for studying the interstellar medium and magnetic field of the Galaxy.

The C-BASS receiver is a combination of a broadband (4.5–5.5 GHz) correlation polarimeter and a pseudo-correlation radiometer (also sometimes known as a continuous-comparison radiometer). The polarimeter correlates right (RCP) and left (LCP) circular polarizations to measure the Stokes Q and U parameters, while the radiometer differences RCP and LCP separately against temperature-stabilized loads to allow accurate total power (Stokes I) measurements.

To obtain full-sky coverage, similar receivers are mounted on two separate telescopes: one at the Owens Valley Radio Astronomy Observatory in California, and the other at Klerefontein, near the MeerKAT Observatory, in South Africa. The survey resolution is 0.73°, with a design sensitivity of < 0.1 mK map rms in Stokes I, Q, and U. Since the contrast between sky and ground temperatures is several hundred Kelvins, limiting scan-synchronous sidelobe pickup to below

the thermal noise level requires that the antennas provide at least 60 dB of rejection in the horizon direction. In addition, given that the polarization fraction of the sky signal may be less than one percent, obtaining accurate polarization angles requires the cross polarization level (after calibration) to be better than -30 dB.

II. Antenna overview and optics design

Due to the availability of suitable antennas at each site, C-BASS uses different antenna designs for the northern and southern surveys. The northern antenna, which was originally designed as a prototype for the NASA Deep Space Network [4], has a 6.1-m primary reflector and was donated to the project by the Jet Propulsion Laboratory. The southern antenna was designed by Mitsubishi for a low-earth-orbit telecommunications satellite ground station. It has a 7.6-m diameter primary mirror, and was donated by Telkom SA Ltd. Both antennas are circularly symmetric and have shaped profiles. The 6.1-m antenna was originally optimized for maximum forward gain using uniform aperture illumination of the primary mirror. The original shaping criteria for the other antenna are unknown. Photogrammetry was used to measure the primary surface shape for both antennas. Since both antennas were originally designed for satellite communication purposes at different frequencies and were not suitable as imaging instruments, the feed and secondary optics were redesigned for this project.

We used Galindo's theory of shaped dual reflectors [5] for the redesign of the secondary mirrors. This provides a set of three differential equations which are solved for the desired boundary conditions. As no closed-form solution is possible, a simple program was written to solve these equations iteratively. The optical design requirements for this astronomical survey were common main beam patterns (up to the first null) from both antennas, low sidelobe and cross polar levels, low blockage and scattering due to the secondary mirror, constant phase in the aperture of the primary mirrors, and, if possible, a common feed horn design for both antennas.

The design procedure started with a ray optics analysis in order to obtain approximate secondary and feed aperture sizes. The first criterion was to limit direct spillover from the feed to the sky and the shadowing of the optics by the feed horn itself, which is to be less than the blockage shadow due to the secondary mirror. The different shapes of the primary surfaces, taken together with these requirements, necessitated different optical configurations – Gregorian (concave ellipsoidal secondary) for the northern antenna and Cassegrain (convex hyperboloidal secondary) for the southern antenna. It was possible, however, to use a common feed horn design. Fig. 1 shows a schematic ray diagram of each design. In both cases our requirements together with the wavelength of the survey caused the diameter of the secondary to be significantly increased compared to the original optics – the new mirrors each subtends a semi-angle of 46.5° from the feed phase centre, at which angle the feed illumination taper is -40 dB at the band centre of 5 GHz.

In the second step the design was optimized using Galindo's design equations. A manual iterative process was used to produce very similar main beam patterns for the two telescopes together with very low sidelobes across the full beam. The cross polar level was relatively independent on the exact design and was mainly set by the cross polar signal level of the feed horn and the fact that our design has unbroken circular symmetry.

Fig. 2 shows the simulated near-in co-polar and cross-polar beams of the two antennas. The beams of the two systems are well matched, allowing for the northern and southern surveys to be combined together with no change of resolution. The main beam efficiency (i.e., the fraction of the total radiated power within the first null) is calculated to be 80%, while the power within 5° (which encompasses most of the diffraction due to the secondary blockage) is 91%. This compares favourably with antennas used for previous total-power surveys, e.g. the Stockert 25-m antenna [6] which has a main-beam efficiency of 55% and a 'full-beam' (within 7°) efficiency of 69%. The high beam efficiency of the C-BASS antennas is due to the lack of scattering structures within the beam, and will result in a much simpler and more accurate conversion from measured power data to true sky temperatures.

III. Antenna design features

To minimize the cross-polar response and far-out sidelobes, three features have been introduced in to the antenna design:

- A very low-sidelobe corrugated feed horn has been designed.
- The secondary mirror is supported by a circular symmetric dielectric foam structure instead of support struts.
- In the case of the 6.1-m antenna, absorbing baffles are mounted around the primary mirrors and also around the secondary mirror. In the case of the 7.6-m antenna, a very high degree of under-illumination is used.

A. Feed horn

The feed horn used for both antennas is a custom design manufactured by Thomas Keating Ltd., with highly suppressed sidelobe levels and low cross-polarization. Drawing upon ideas designed to minimize reflections in quasi-optical circuits [7], the corrugated horn has a cosine-squared profile designed to generate a significant amount of HE12 mode which is followed by a phasing section which brings the HE12 mode into phase with the dominant HE11 mode. The combination of these modes provides an aperture field with low edge taper which translates into a pattern with very low sidelobes.

Modal matching predictions of the low sidelobe horn for C-BASS from CORRUG [8] as well as modelling and measuring patterns for other similar horns at much higher frequencies [9] show that this design of corrugated horn retains its very low sidelobe and cross-polar performance over large bandwidths. Our design is optimized for 5.0 GHz, at which the peak sidelobe level is -40 dB relative to the boresight level and the peak cross-polarization is -47 dB. At the band edges at 4.5 GHz and 5.5 GHz the sidelobe levels degrade to -32 dB and cross-polarization to -33 dB, which is still acceptable performance over a 20% bandwidth. The pattern of the feed

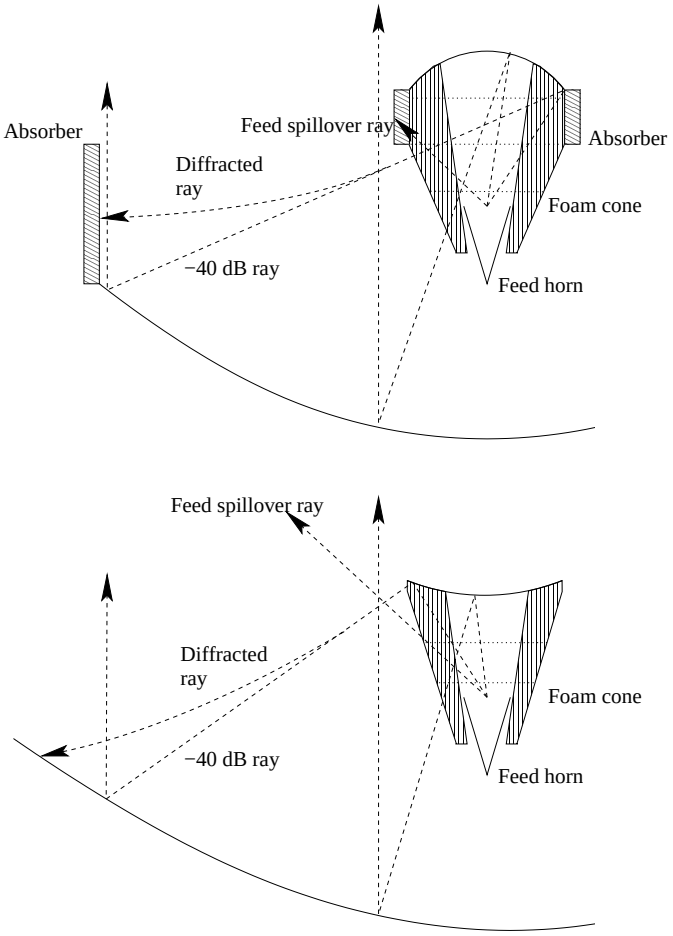

Fig. 1. Schematic ray diagrams (not to scale) of (top) the northern 6.1-m antenna and (bottom) the southern 7.6-m antenna. In the northern antenna both direct spillover from the feed and diffraction spillover around the primary mirror edge are blocked by absorbing baffles. In the southern antenna, primary spillover is limited by the under-illumination of the larger antenna; direct spillover past the secondary cannot be further limited due to the Cassegrain geometry. Dotted lines in the foam cones indicate glue joints which are traversed by free-space rays.

horn at 5.0 GHz, as predicted by CORRUG, is shown in Fig. 3.

The horn aperture radius is 113 mm, and it produces an illumination at the edge of the secondary mirror of -40 dB. The horn is manufactured in three corrugated segments, which are bolted to the outside of the receiver cryostat, and two smooth conical segments which are integral to the outer (room temperature) and intermediate (40 K) shells of the cryostat. The outer smooth section also incorporates a Mylar vacuum window and a Zotefoam plug to block infrared loading. The horn terminates in a specially designed four-probe orthomode transducer [10] which generates left and right circular polarizations. In our facilities we could only measure the near-field beam pattern at 3 m distance. This measurement is shown alongside the equivalent near-field simulation in Fig. 4.

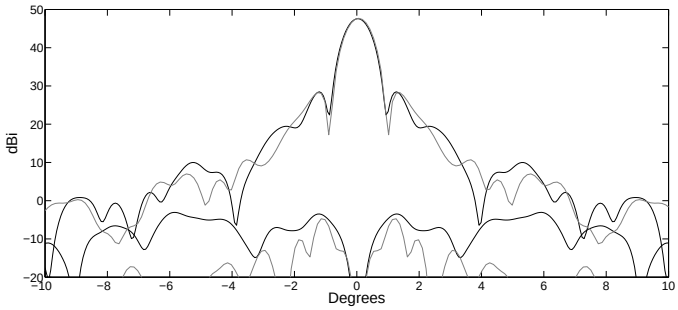

Fig. 2. Simulation of the co- and cross-polar forward beams of the 6.1-m antenna (black) and the 7.6-m antenna (grey).

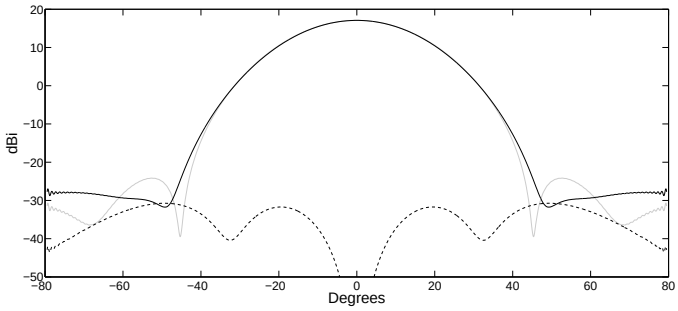

Fig. 3. Simulated feed horn pattern at 5 GHz; E-plane (grey), H-plane (black) and cross-polar (dotted black).

B. Secondary mirror and support

In a circularly symmetric design, secondary support struts block and scatter signals in a manner which is difficult to control. The break in symmetry due to the struts results in elevated levels of cross-polar signals. In addition, the scattered signals increase the system noise via ground pickup in a way which is dependent on the pointing direction of the antenna. For sensitive polarization experiments it is essential to minimize the effect of the secondary support. One option is to use offset antennas with no blocking. However, this can increase costs significantly, especially since in our case two circularly symmetric antennas were readily available. An alternative method is to support the mirror using a material which is effectively transparent at the frequency of operation, i.e., has both low loss and low refractive index. We chose the material Plastazote from Zotefoams Ltd, which at low microwave frequencies is almost fully transparent and therefore can be used to support the secondary mirror without blocking or scattering the signal.

1) Secondary support material characteristics: Plastazote is a closed-cell expanded polyethylene foam formed by the vacuum expansion of heated polyethylene sheets that have had nitrogen diffused into the solid phase under pressure. Two different grades are available, using either low density (LD) or high density (HD) polyethylene as the starting material. HD polyethylene (HDPE) is only slightly denser (930 – 970 kg m^{-3} than LDPE (910 – 930 kg m^{-3}) but is considerably stiffer due to reduced branching of the polymer chains and consequently higher intermolecular forces. Depending on the amount of infused nitrogen, the foam density after expansion can be between 15 and 115 kg m^{-3}. The dielectric constant of

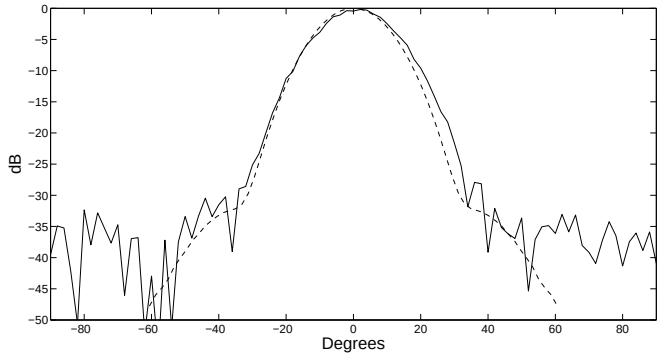

Fig. 4. Feed horn near-field (3 m) pattern at 4.5 GHz; measurement (black), simulation (dotted black).

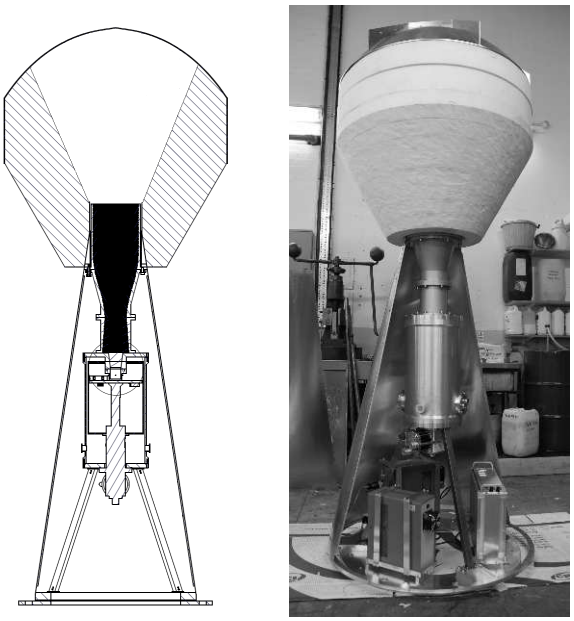

Fig. 5. Receiver, feed horn, secondary support cone and secondary mirror in a drawing (left) and during assembly (right).

solid LDPE and HDPE is about 2.3 and the loss tangent, $\tan\,\delta$, is 3.1×10^{-4}. We measured the dielectric constant and loss of samples of the foam for various density and material grades by filling a rectangular waveguide section with a foam sample and measuring the change in phase and amplitude compared to an empty waveguide, using a vector network analyzer. We found that the results were consistent with a simple scaling of the properties with solid fraction of the foam, i.e., the dielectric constant was given by

$$\varepsilon_{\rm foam} - 1 = (\rho_{\rm foam}/\rho_{\rm solid})(\varepsilon_{\rm solid} - 1)$$

and the loss tangent was given by

$$\tan(\delta)_{\rm foam} = (\rho_{\rm foam}/\rho_{\rm solid})\tan(\delta)_{\rm solid}.$$

The foam can be glued to itself and to metals with standard adhesives, and can also be heat welded to itself. Heat welding is used to build up the basic manufactured sheets, which are around 30 mm thick, into laminated blocks of thickness up to 300 mm (limited by the size of the heat welding equipment). We used an impact adhesive (Evostick TX528) to join together blocks to make larger structures. This adhesive was tested for RF properties by inserting glued foam samples into a waveguide, with the glue joint across the waveguide, and testing on a vector network analyzer. No change in average transmission compared to a single unglued piece of foam was detected at the level $<$0.05 dB.

2) Secondary support design: A drawing of the receiver, secondary support cone and secondary mirror for the 6.1-m Gregorian system is shown in Fig. 5. Initially, the foam cone was constructed out of 120-mm thick sheets of LD45 (LDPE base material with a density of 45 kg m^{-3}), glued together in layers perpendicular to the optic axis, and cut to shape with a bandsaw. This grade of foam was used for the secondary mirror supports in the Cosmic Background Imager 2 instrument [11]. The foam cone was glued (using impact adhesive) to a hollow aluminium conical insert which mounts to a flange on the outside of the feed horn. Adjustment screws at this interface allow a small amount of motion in focus and tip-tilt. The secondary mirror was glued to the top of the foam cone.

After approximately 18 months in service it became apparent that some of the foam-to-foam and foam-to-metal joints were beginning to fail due to weathering and mechanical load. We decided to re-make the cone using HD grade foams to increase the stiffness of the structure, and to reduce the load on the most vulnerable joints. The base section of the new cone, which bears the largest mechanical forces and transmits them to the telescope structure, was made from a single piece of HD115, which was available in heat-laminated blocks 300 mm thick. HD115 has a flexural modulus of 23 MPa, compared to 1.0 MPa for LD45. The remainder of the cone was made from blocks of HD30, which has a flexural modulus of 3.6 MPa, higher than that of LD45 despite its lower density. The base section was glued to the aluminium insert using Araldite 2005 space-filling epoxy resin, which is stronger and more weather-resistant than the impact adhesive. Epoxy was also used for fixing a new carbon-fibre secondary mirror (see below) to the top of the cone. The epoxy was measured to have significantly higher RF loss than the impact adhesive; this is not important for the base joint (which is outside the beam) or the mirror joint (which is a reflective surface and therefore has zero electric field close to the surface), but would be significant for the foam-to-foam joints which the beam crosses in free space. We therefore retained the low-loss impact adhesive for these joints but protected the joint edges against weathering by wrapping the exposed cone structure in a thin polyethylene membrane. Due to the thicker foam sections being available only three such joints were needed, compared to eight in the previous design. Using lower density foam for the bulk of the structure and a lighter mirror also significantly reduced the stress on the joints.

3) Secondary mirror design: Secondary mirrors of different shapes were required for the two antennas – a deep concave ellipsoidal mirror for the 6.1-m antenna, and a shallow convex hyperboloidal mirror for the 7.6-m antenna. To minimize the weight that has to be supported by the foam structure, a lightweight design was developed. Initially for the 6.1-m antenna a light-weighted machined aluminium mirror was used.

The mirror was constructed from seven aluminium segments, a central section and six identical petals, bolted together via backing ribs. The back and sides of each mirror segment were machined down to 3 mm thickness, and the whole mirror had a mass of 12 kg. This mirror was used with the initial foam support made from LD45. When this support was re-made using HD foam we also decided to change to a carbon-fibre mirror, in order to further reduce the mechanical load. The mirror was made to exactly the same design as the first mirror, using five layers of prepreg carbon fibre weave for each segment, laid up on a machined aluminium mould, and cured under pressure in an autoclave. Reflectivity measurements on carbon fibre samples showed a reflection loss 1 per cent worse than solid aluminium, which would have added about 3 K to the total system temperature, a significant effect. We therefore covered the front surface with 3M aluminium adhesive tape to provide a metallic reflecting surface. The total mass of the carbon fibre mirror was about 2 kg. The maximum deflection of this new cone/mirror assembly under gravitational load was less than 0.1 mm, which corresponds to a shift in beam pointing of 10 arcsec. This is negligible compared to the beam size of 0.73°. For the 7.6-m antenna secondary we follow the original manufacturing method of directly machining seven mirror segments from aluminium. This is significantly cheaper for a one-off production and, in combination with the HD foam, results in negligible shift in the beam pointing due to gravitational loading.

4) Performance: Possible contributions to the overall system noise from the foam cone were estimated from measurements using the C-BASS receiver. The total system noise power out of the cryogenic receiver was measured with the bare feedhorn pointing at the sky, with the secondary optics in place, and with the feed terminated with a room-temperature absorber. The noise power contributions of the receiver, sky and optics were estimated from comparisons between the power measured from the sky, a room-temperature absorber, and absorber cooled to 77 K with liquid nitrogen. The excess power attributable to the secondary optics (including loss in the foam and ground pick-up from spillover around the primary) was no more than 1 K. Limits on the scattering produced by the foam are given by the agreement between measured and calculated far-out sidelobes (see Section IV below). The measurements were repeated for the new foam cone made from HD foam, with identical results. If we had used a conventional secondary support system, GRASP-9 simulations of a representative 4-strut support show that the expected blockage would be around 5% of the total power, resulting in a spillover contribution of 5 – 7 K, which would be highly position-dependant and would result in significant scan-synchronous pickup during survey observations.

C. Absorbing baffles

Signal spillover past the primary and secondary mirrors produces far-out sidelobes. This can increase the system temperature when these sidelobes point at bright sources or the ground. In addition, these sidelobes can be strongly polarized and induce changes in the intensity and polarization signal as the pointing of the antenna varies. Far-out sidelobes due to spillover past the edge of the primary mirror can be significantly reduced by mounting an absorber-lined cylindrical baffle around the rim of the primary mirror [12]. We have taken this idea further and also fitted the secondary mirror (on the 6.1-m antenna) with an absorbing baffle to block spillover past the secondary mirror direct to the sky. The structure is shown in Fig. 1 and Fig. 6. Due to the different ray geometry a baffle around the secondary is only possible with a Gregorian system and not with a Cassegrain system.

Fig. 6. The 6.1-m antenna at the Owens Valley Radio Astronomy Observatory with the new secondary support structure and the absorber-lined baffle around the rim of the primary and around the upper part of the foam secondary support structure.

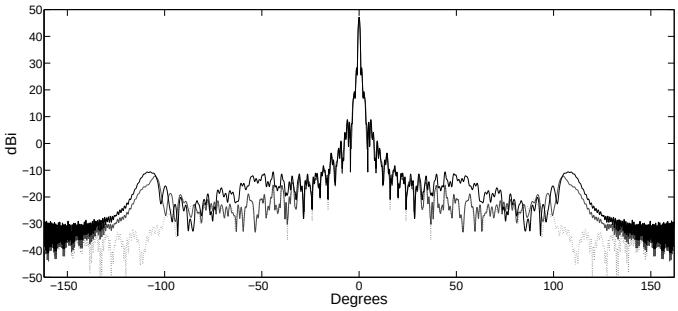

Fig. 7. Simulated beam pattern of the 6.1-m antenna at 4.5 GHz, without baffle (black), with secondary baffle only (grey) and with both baffles (dotted black) attached.

The absorbing material radiates at ambient temperature and therefore increases the system temperature. However, this temperature component is stable with pointing and unpolarized, and therefore produces no changing signal as the antenna scans the sky. Provided the fraction of the total illumination intercepted by the absorbers is kept small, the benefit of reducing scan-synchronous pickup outweighs the increase in system noise.

We found that a reduction in spillover sidelobe level of 17 dB at 4.5 GHz could be achieved with an absorber of height 0.8 m above the rim of the 6.1-m primary. This results in a temperature load contribution of 0.7 K. The temperature contribution from the secondary baffle is 0.2 K. For the 7.6-m antenna this would be considerably less, 0.1 K from the primary baffle, due to the lower edge illumination of the larger antenna. In practice the benefit of the absorbing baffle for the 7.6-m antenna is marginal given the very strong

TABLE I
ANTENNA CHARACTERISTICS AND SIMULATED PERFORMANCE

Performance at 5 GHz	6.1-m antenna	7.6-m antenna
FWHM	0.73°	0.73°
Gain	47.6 dBi	47.7 dBi
First sidelobe level	−19.1 dB	−19.3 dB
Cross-polar level	−51 dB	−52 dB
Primary mirror radius	3.048 m	3.835 m
Primary illumination radius (−40 dB)	2.96 m	3.25 m
Secondary mirror radius	0.51 m	0.50 m
Antenna type	Gregorian	Cassegrain
Primary baffle depth	0.80 m	–
Secondary baffle depth	0.30 m	–
Primary baffle temp. contribution	0.7 K	–
Secondary baffle temp. contribution	0.2 K	–
Beam efficiency (power within ±5°)	91.9%	91.3%
Main beam efficiency (power within first null)	80.0%	80.0%

under-illumination of the primary, and we have elected not to implement it.

The full beam patterns for the two antennas including the effect of the absorbing baffles on the 6.1-m antenna were simulated using GRASP9. To allow reasonable meshing of the surfaces representing the absorbers in GRASP9 it was necessary to slightly displace them from the mirror surfaces. This is not expected to have any significant effect on the calculated beams. The characteristics of both antennas are summarized in Table I. Despite the different antenna sizes and primary illumination radii, the main beams and first sidelobe levels are identical for both antennas. The cross polar signal levels are also very similar. The effect of the primary and secondary baffles is shown in simulation in Fig. 7. Here the results are shown at 4.5 GHz, since the effect is strongest at the lower edge of the observing band. The sidelobes at 50° are due to spillover past the secondary mirror and are suppressed by the baffle around the secondary. The spillover past the primary at about 110° is suppressed by the primary baffle.

The secondary baffle is implemented by wrapping foil-backed absorber (Advanced ElectroMagnetics AEL-0.375) around the cylindrical section of the foam secondary support structure. For the primary baffle, a structure of curved aluminium sheets supported on struts connected to the outer rim of the primary reflector was constructed, and the absorber glued to the inner face of the sheets.

IV. ANTENNA PERFORMANCE

A. Main beam measurements

The 6.1-m antenna can only be pointed to a minimum elevation of 13°, and hence cannot be easily pointed to an artificial source in the far field. We therefore measured the main beam using an astronomical source and the radiometer backend built for the C-BASS survey, which measures the difference between the power received by the feed horn and that from a stabilized cold load. The antenna was repeatedly swept backwards and forwards in azimuth about the position of the radio source Cassiopeia A (Cas A), which is one of the brightest compact radio sources in the northern sky (670 Jy at 5 GHz [13]). Cas A is approximately 5 arcmin in diameter, and thus much smaller than the beam (FWHM 44 arcmin). A linear fit was removed from each scan to remove the effect of changing airmass during the observation and also to remove the diffuse Galactic emission near Cas A (around 1 per cent of the peak source brightness). The data were then stacked as a function of offset from the nominal source position. Fig. 8 shows the stacked data, overlaid with the simulated main beam lobe and first sidelobes.

At the time of these observations, the actual position of the secondary mirror was measured to be raised 5 mm higher than nominal, so for direct comparison the simulation of the main beam was recalculated with this offset included in the geometry. The simulated beam was calculated at three frequencies, 4.5, 5.0 and 5.5 GHz. We modeled the variation of the flux density of Cas A with frequency as ν^α, where ν is the frequency and α is the spectral index, which for Cas A is -0.767 [13]. The simulated beam was formed by weighting each narrow-band simulation by the expected flux density and then averaging over the three frequencies. Fig. 8 shows excellent agreement between the simulated beam and the measurement of the main beam and first sidelobe.

We also used these measurements to place a limit on the cross-polar levels of the main beam. In Fig 8 we show the measured polarization ($P = (Q^2 + U^2)^{1/2}$) response to the (nominally unpolarized) source Cas A. We subtracted the best-fitting scaled co-polar beam from the scanned P data, which represents polarization leakage ($I \rightarrow P$) in the polarimeter, plus any intrinsic polarization of the source. The appropriate scaling was approximately 1% of the co-polar peak. Cross-polarization in the optics is expected to have a quite different beamshape, with a null at the centre and peaks near the first null of the co-polar beam. No such beamshape is evident in the plots at the level of $\sim -20\,\mathrm{dB}$ down from the peak. The expected level of cross-polarization is $< -50\,\mathrm{dB}$ relative to the peak co-polar response (see Fig 2), much smaller than this measured limit. With the southern 7.6-m telescope, which can be pointed to the horizon and hence to an artificial source, we expect to make a much more sensitive measurement of the optical cross-polarization.

B. Far-out sidelobe measurements

For far-out sidelobe measurements, a ground-based 5 GHz CW signal source was used at a distance of 4.5 km, in the antenna's far field. Due to pointing limitations of the telescope mount we were only able to map the sidelobe pattern between boresight angles of 13° – 82° and 95° – 163°. The signal source was switched on and off at 0.7 Hz to allow discrimination between the test signal and ground pick-up and background sources. Fig. 9 shows the beam pattern measurement compared to the simulation results at 5 GHz, without baffles. Since the exact distance and power level of

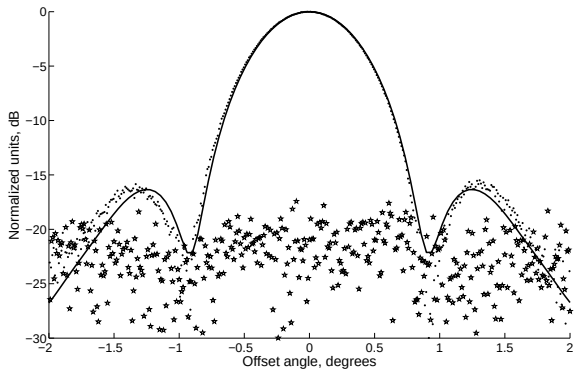

Fig. 8. Simulated main beam (solid line), averaged over the system bandwidth, and measured beam (dots) measured from azimuth scans on the astronomical source Cas A. Stars show the polarized ($P = (Q^2 + U^2)^{1/2}$) response to this unpolarized source, after subtracting a leakage term due to imperfections in the polarimeter. This is an upper limit on the degree of cross-polarization in the optics – the expected level is $< -50\,\mathrm{dB}$.

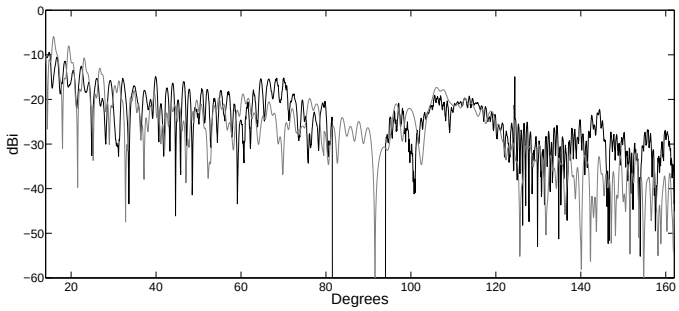

Fig. 9. Measured (black) and simulated (grey) beam pattern of the 6.1m antenna without baffles between 13° and 163° at 5 GHz. There is no measured data between 82° and 95°. Note that the vertical axis is in dBi and the peak of the main beam is at $+47.6$ dBi.

the signal source was known, the absolute gain of the antenna pattern in dBi could be calculated. Fig. 9 shows very good agreement between measurement and simulation even at signal levels of more than 60 dB below the antenna's forward gain.

Two further measurements were conducted including the absorbing baffle around the secondary, and around both the secondary and primary, as discussed in section III. Fig. 10 compares the three measurements with and without the absorbing baffles. There is a clear reduction of sidelobe levels at 50° and 110°. The backlobe response (at angles greater than 100°) is reduced by 10–20 dB and the absolute level is reduced to more than 90 dB below the main beam. Measurements were made both with the original aluminium secondary mirror and LD foam cone, and with the replacement carbon-fibre mirror and HD foam cone, with identical results.

V. Conclusions

We have presented the development of two circularly-symmetric radio antennas which have been modified to meet the special needs of high polarization purity and low signal contamination for an all-sky survey at 5 GHz. These needs have been met by three key design features. First, a low sidelobe and low cross-polarization feed horn has been developed. Second, the secondary mirror is supported by a transparent circular Zotefoam cone without metal struts, and third, absorbing baffles have been fitted to minimize spillover. We have shown simulated results and compared these to measurements of one of the two antennas, the 6.1-m antenna at the Owens Valley Radio Observatory. In particular, the foam secondary support cone makes only a small contribution to the system temperature and is a good option to conserve polarization purity in a circular symmetric design without the need for metal support struts. The use of absorber around the rims of both the primary and secondary mirrors is shown to decrease significantly the sidelobes due to spillover around both mirrors.

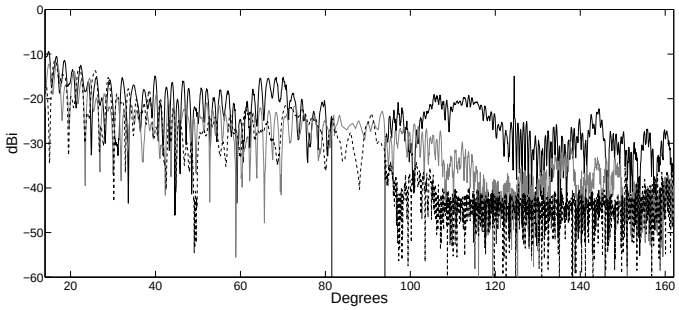

Fig. 10. Three far-out sidelobe measurements between 13° and 163° at 5 GHz without baffle (black), with secondary baffle only (grey) and with both baffles (dotted black).

Acknowledgment

The authors would like to thank the staff of the Mechanical Engineering group in the Oxford University Department of Physics, particularly Mike Tacon, Paul Rossiter and Matthew Brock, for the construction of the C-BASS optical components. We also thank the staff of the Owens Valley Radio Astronomy Observatory, particularly Russ Keeney, for support of the operations of the C-BASS North telescope.

References

[1] O. G. King *et al.*, "The C-Band All-Sky Survey: instrument design, status, and first-look data," in *Society of Photo-Optical Instrumentation Engineers (SPIE) Conference Series*, vol. 7741, 2010.

[2] C. L. Bennett *et al.*, "The Microwave Anisotropy Probe Mission," *ApJ*, vol. 583, pp. 1–23, Jan. 2003.

[3] Planck Collaboration, "Planck Early Results: The Planck mission," *A&A*, vol. 536, p. A1, 2011.

[4] W. A. Imbriale and R. Abraham, "Radio frequency optics design of the deep space network large array 6-meter breadboard antenna," Jet Propulsion Laboratory, Pasadena, CA, The Interplanetary Network Progress Report, vol. 42-157, May 15 2004.

[5] V. Galindo, "Design of dual-reflector antennas with arbitrary phase and amplitude distributions," *IEEE Trans. Antennas and Propagation*, vol. 12, no. 4, pp. 403–408, 1964.

[6] W. Reich, "A radio continuum survey of the northern sky at 1420 MHz. I," *A&AS*, vol. 48, pp. 219–297, May 1982.

[7] P. S. Cruckshank, D. R. Bolton, D. A. Robertson, R. J. Wylde, and G. M. Smith, "Removing standing waves in quasi-optical systems by optimal feedhorn design," in *IRMMW-THZ Conference Digest*, Sep 2007, pp. 941–942.

[8] Corrug. SMT Consultancies Ltd. [Online]. Available: http://www.smtconsultancies.co.uk/products/corrug/corrug.php

[9] Thomas Keating Ltd, "Ultra-Gaussian Corrugated Horns," Tech. Rep. [Online]. Available: http://www.terahertz.co.uk/index.php?option=com_content&view=article&id=189&Item

[10] P. K. Grimes, O. G. King, G. Yassin, and M. E. Jones, "Compact broadband planar orthomode transducer," *Electronic Letters*, vol. 43, pp. 1146–1148, 2007.
[11] A. C. Taylor *et al.*, "The Cosmic Background Imager 2," *MNRAS*, vol. 418, pp. 2720–2729, 2011.
[12] R. Dybdal and H. King, "Performance of reflector antennas with absorber-lined tunnels," in *Antennas and Propagation Society International Symposium, 1979*, vol. 17, Jun 1979, pp. 714 – 717.
[13] Y. A. Hafez *et al.*, "Radio source calibration for the very small array and other cosmic microwave background instruments at around 30 GHz," *MNRAS*, vol. 388, pp. 1775–1786, 2008.

Christian M. Holler was born in southern Germany in 1973. He studied physics at the Ludwig-Maxmilians-Universität in Munich, Germany and received his PhD in the field of astrophysics and instrumentation at the Cavendish Laboratories, Cambridge University, UK in 2003. After successfull entrepreneurial work he joined the experimental cosmology group at the University of Oxford as a postdoctoral research assistant, where he was involved in several instrumentation projects. In September 2009 he was appointed a Professor at the University of Applied Sciences in Esslingen, Germany.

Angela C. Taylor was born in Dartford, UK in 1975 and studied Natural Sciences at Cambridge University, earning a PhD in astrophysics at the Cavendish Laboratory Cambridge in 2002. She continued to work in the field of astrophysics and instrumentation as a postdoctoral research assistant at the Cavendish Laboratory until 2005 when she moved to the University of Oxford as a founding member of the experimental cosmology group. Since January 2005 she has been an STFC Postdoctoral Research Fellow and then a Royal Society Dorothy Hodgkin Research Fellow working on a range of experimental cosmology projects at the University of Oxford.

Michael E. Jones was born in Wrexham, UK, in 1966 and studied Natural Sciences and Electrical Science at Cambridge University. He obtained a PhD in Radio Astronomy at the Cavendish Laboratory, Cambridge in 1990 and subsequently worked there as a Research Associate and Senior Research Associate. In 2005 he was appointed first as a Lecturer and then as Professor of Experimental Cosmology at the University of Oxford Department of Physics.

Oliver G. King was born in Bedford, South Africa in 1983. He studied Physics and Electronics at Rhodes University in Grahamstown, South Africa. He obtained a DPhil in Astrophysics at the University of Oxford in 2009, where he worked on radio instrumentation. He moved to the California Institute of Technology in Pasadena, California in late 2009 to take up a Keck Postdoctoral Fellowship. At Caltech he leads astrophysics instrumentation projects from radio to optical wavelengths.

Stephen J. C. Muchovej was born in southeastern Brasil in 1979. He earned a Bachelors degree in physics and astronomy from the University of California, Berkeley. He earned his PhD in 2008 from Columbia University in the field of astrophysics with a focus on instrumentation and experimental cosmology. He is currently a National Science Foundation fellow at the California Institute of Technology.

Matthew A. Stevenson was born in Winnipeg, Manitoba, Canada, in the early 1980s. He received his BSc in Astronomy and Physics from University of Victoria, British Columbia, Canada. Since 2006 he is a PhD student in Astronomy at the California Institute of Technology.

Richard J. Wylde was born in London in 1958 and educated at Eton and Sidney Sussex College, Cambridge and studied Natural Sciences. He joined Queen Mary College, University of London, and received the Ph.D. degree in physics in 1985. He is a Fellow of the Institution of Engineering and Technology. He is currently an Honorary Reader in the School of Physics and Astronomy, University of St. Andrews, Scotland, and he manages both Thomas Keating Ltd. precision engineers, and QMC Instruments Ltd. His research interests lie in the design of THz systems for use in thermonuclear plasma diagnostics, observational cosmology, astronomy, electron-spin-resonance spectroscopy and atmospheric remote sensing.

Charles Copley was born in Pietermaritzburg, South Africa in 1982 and educated at Michaelhouse, Rhodes University and the University of Cape Town. Since 2010 he has been pursuing a DPhil at the University of Oxford, with a focus on instrumentation.

Richard J. Davis was born in March, UK in 1949 and studied Natural Sciences at Cambridge University, earning a PhD in radio astronomy at the University of Manchester in 1975. He continued to work in the field of astrophysics and instrumentation as an SERC fellow and then a University PDRA at Jodrell Bank till 1978 and then as an academic member of staff.

Timothy J. Pearson is a senior research associate in radio astronomy at the California Institute of Technology. He received his Ph.D. from the University of Cambridge in 1977. His research interests include radio astronomy, interferometry, active galactic nuclei, and the cosmic microwave background radiation.

Anthony C. S. Readhead is the Barbara and Stanley R. Rawn, Jr., Professor of Astronomy at the California Institute of Technology, and Director of the Owens Valley Radio Observatory and a Senior Research Scientist at the Jet Propulsion Laboratory. He studied physics and mathematics at the University of the Witwatersrand in South Africa, and conducted Ph.D. research on active galaxies and interplanetary scintillation at the Cavendish Laboratory, University of Cambridge. He was elected to the National Academy of Sciences and the American Academy of Arts and Sciences in 1995.